Available online at www.sciencedirect.com

ScienceDirect

Procedia Social and Behavioral Sciences 20 (2011) 398–405

Procedia Social and Behavioral Sciences

14th EWGT & 26th MEC & 1st RH

Lattice thermodynamic model for vehicular congestions

Milan Krbálek[a,*], Katarína Kittanová[a]

[a]*Faculty of Nuclear Sciences and Physical Engineering, Czech Technical University in Prague, Trojanova 13, Prague 12000, Czech Republic*

Abstract

We introduce the spatially-discrete time-continuous particle system whose intelligent elements are interconnected by the psychological short-ranged interactions and stochastically influenced by the nonzero level of psychological strain. Dividing the circular lattice into the regions of different strain-levels we detect the strong traffic congestion propagating through the entire system. As follows from the relevant statistical analysis of traffic data, both the macroscopic and microscopic structures of the above-mentioned cellular model are in a good agreement with those observed in freeway samples.

Keywords: cellular models; thermal-like traffic model; clearance distribution; vehicular traffic; traffic congestion

1. Terminus a quo

The first attempts to describe certain vehicular ensembles systematically, i.e. using mathematical techniques, were noticed more than seventy years ago. Indeed, in 1935 there was published the first scientific paper (Greenshields, 1935) on elementary relations among traffic quantities. Bruce Douglas Greenshields – author of this text – was probably the first man who carried out the traffic flow measurements (using photographic measurement methods) and predicted the linear speed-density relation. Many mathematicians, physicists, or traffic engineers have followed up to his pioneering work since then. Recently, knowledge on behavior of traffic systems is very extensive (see reviews May, 1990; Chowdhury, 2000; Helbing, 2001 or Kerner, 2004) as well as mathematical or/and physical methods used for traffic modeling.

Many contemporary treatises dealing with physics of traffic discuss possibilities for application of thermodynamic approaches to the traffic modeling (see Krbálek, 2004; Sopasakis, 2004; Krbálek, 2007; Mahnke, 2007; Krbálek, 2008 and Krbálek, 2009). These attempts have been partially successful predominantly if the local thermodynamics was adopted. Specifically, introducing the socio-physical particle scheme with mutual interactions described by the repulsive forces among the subsequent elements one can obtain surprisingly good analytical estimations for microscopic traffic quantities or their statistical distributions (see Krbálek, 2007 and Krbálek, 2009).

* Corresponding author. Tel.: +420-224-358-550
E-mail address: milan.krbalek@fjfi.cvut.cz

1877–0428 © 2011 Published by Elsevier Ltd. Selection and/or peer-review under responsibility of the Organizing Committee
doi:10.1016/j.sbspro.2011.08.046

In spite of the fact that the initial scheme is of thermodynamic substance the alternative formulation of the model may potentially lead to the effects of crowding. Investigation of that hypothesis is the subject of the next sections.

2. Traffic model formulation

In this section we introduce an original variant of numerical/analytical traffic simulator whose background is space-discrete. Contrary to the famous cellular automata: Nagel-Schreckenberg's model (see Nagel, 1992 for details), Fukui-Ishibashi's (see Fukui, 1996), and totally asymmetric simple exclusion process (see Derrida, 1992), our simulation scheme is of thermal-like nature and takes some psychological aspects of traffic into account.

Consider a circular cellular freeway of circumference n divided into m equivalent cells of the same length (see Figure 1). Above that, define n dimensionless vehicles placed inside the lattice so that each cell can be occupied by one car only. Thus, every particle (car) is unambiguously described by the corresponding angle coordinate $\vartheta_i \in [0, 2\pi)$ which is understood as a discrete quantity, i.e. for every $i = 1,2, \dots, n$ it holds

$$1 \leq \varepsilon_i = 1 + \frac{m\vartheta_i}{2\pi} = 1 + \left\lfloor \frac{m\vartheta_i}{2\pi} \right\rfloor \leq m, \qquad (1)$$

where ε_i represents the numerical order of cell that is occupied by the ith particle and brackets stand for the lower integer-part of a given real number. Denote $\vartheta_{n+1} = \vartheta_1 + 2\pi$, for convenience. Thus, the entire system is developing in $2n$-dimensional phase space whose points are described by the vector $\vec{\vartheta} = (\vartheta_1, \vartheta_2, \dots, \vartheta_n)$ of positions and vector $\vec{v} = (v_1, v_2, \dots, v_n)$ of velocities. Introducing the two-body repulsion potential $V(r_i) = r_i^{-1}$, where

$$r_i = \frac{n}{2\pi}(\vartheta_{i+1} - \vartheta_i) \qquad (2)$$

represents a circular distance between $(i+1)$th and ith particles, the associated socio-physical Hamiltonian of the system introduced reads

$$\mathcal{H} = \frac{1}{2}\sum_{i=1}^{n}(v_i - \bar{v})^2 + C\sum_{i=1}^{n} V(r_i). \qquad (3)$$

Here the former reflects the fact that drivers moving with optimal velocity $\bar{v}$ (being sufficiently far from other cars, where $V(r) \approx 0$), do not accelerate/decelerate. The latter summarizes all two-body repulsive potentials in the global potential energy

$$U = \sum_{i=1}^{n} V(r_i) = \sum_{i=1}^{n} \frac{1}{r_i}. \qquad (4)$$

Its specification follows directly from the previous works (Krbálek, 2004, 2007). C is a positive constant.

In fact, the above-mentioned definition is deterministic and does not reflect stochastic features of vehicular systems. Therefore we introduce the thermodynamic alternative of the model (being inspired by the articles Sopasakis, 2004; Helbing, 2004; Helbing, 2006; Krbálek, 2007) where the entire system is exposed to a random noise of thermodynamic origin. Level of such an external fluctuation-impact used to be quantified (in statistical disciplines) by the thermal parameter T − usually called a thermodynamic temperature. In this article we will use the reciprocal value $\beta = (k_B T)^{-1}$ instead. Constant k_B is the usual Boltzmann factor. We add that the thermodynamic component leads the systems to the state of statistical balance where the statistical distributions are fixed, in spite of the fact that individual quantities (locations, velocities, headways) are varying.

In the socio-physical disciplines (see Helbing, 1995) the thermal parameter $\beta \geq 0$ can be interpreted as a psychological coefficient describing a level of the mental pressure under which the agent (here driver) is while driving his/her car. Such a mental strain coefficient β can be defined either globally (which means that all drivers are under the same strain) or individually (β is an individual property of each driver) or locally (for chosen part of

freeway, β is fixed to a constant value). Implementing such a thermal component into the originally deterministic system we are obtaining the chaotic ensemble whose steady state is described statistically. It means that the microscopic quantities (gaps among the cars, velocities of single vehicles, time intervals among the subsequent cars and so on) measured in the steady state are determined by means of associated probability densities. This fact fully corresponds to the ascertainments observed in traffic experiments (see Sugiyama, 2008 and Orosz, 2009).

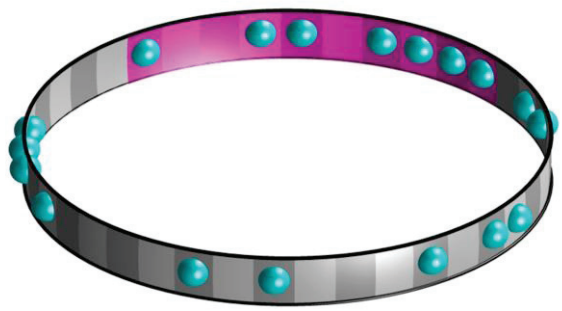

Figure 1. Particles (Cars) on a Multi-Segment Cellular Ring. The locations of particles are discretized and subjected to the simple exclusion rule, which means that every cell can be occupied by one car only. The ring is divided into the regions of different psychological loads quantified by the different values of strain-parameter β.

For purposes of this article we will consider a locally-depending-strain version of the previously-mentioned model (see also Figure 1). It means that we divide the whole circular freeway into two segments (similarly to the approach in Nishimura, 2006). In the first one (ranging from zero angle $\varphi = 0$ to φ_c) the mental strain coefficient is preset to β_0, whereas in the second segment (ranging from φ_c to $\varphi = 2\pi$) we choose β_c. We call this part the critical region. That choice corresponds to the empirical findings (see Krbálek, 2009) that the different traffic phases (especially free vs. congested regimes of traffic) show significantly dissimilar microstructures (i.e. different probability densities for individual traffic quantities).

3. Mean-segment approximation of the MSCTT-model

If aiming to predict the steady-state of our multi-segment cellular thermal-like model (abbreviated as MSCTT-model) described above we introduce the corresponding partition function which is of the form

$$Z_n = \sum_{v_i} \sum_{\vartheta_i} \delta\left(2\pi - \sum_{i=1}^{n} (\vartheta_{i+1} - \vartheta_i)\right) \prod_{i=1}^{n} \exp\left[-\frac{\beta_i}{2}(v_i - \bar{v})^2\right] \prod_{i=1}^{n} \exp\left[-C\beta_i V\left(\frac{n}{2\pi}(\vartheta_{i+1} - \vartheta_i)\right)\right] \qquad (5),$$

where temperature-like parameter β_i is chosen from the set $\{\beta_0, \beta_c\}$ according to the actual position of ith agent/particle. We remark that symbol $\delta(x - \mu)$ represents the generalized function called Dirac delta-function.

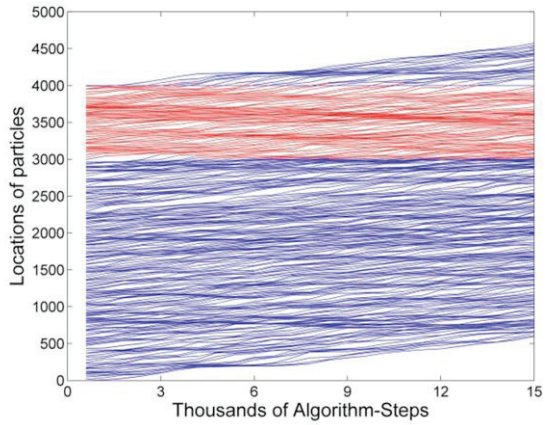

Figure 2. Trajectories of the Particles in Multi-Segment Thermal-like Cellular Model. The segments of different strain-coefficients are distinguished by colours. In the specific regions one can detect the local traffic congestions propagating through the entire system.

Restringing this partition function to the inner part (being sufficiently far from the segment boundaries) of the specified ring-segment (where β_i is constant) and eliminating the velocity part of Z_n one can approximate the time-evolution in the chosen segment by the one-dimensional thermodynamic gas. It means that the global steady-state of the above-mentioned system can be approximated by the local thermal equilibria of the partial systems (corresponding to the individual segments of the ring). Now, applying certain routines of statistical physics (see [Krbálek 2007] or [Bogomolny 2001]) we predict that steady state of our multi-segment cellular model should be described by the following statistical description. The probability density for distance among successive particles in the steady states reads

$$\wp(r) = A\,\theta(r)\exp\left[-\frac{\beta}{r} - Br\right], \qquad (6)$$

where the symbol $\theta(r)$ corresponds to the Heaviside step-function and two constants

$$B = \beta + \frac{3 - \exp\left[-\sqrt{\beta}\right]}{2}, \qquad A^{-1} = 2\frac{\beta}{B}K_1\left(2\sqrt{\beta B}\right) \qquad (7)$$

assure the proper normalization and the scaling to the mean distance equal to one (in consonance with the original formulation of the model). The function $K_1(x)$ represents the modified Bessel's function of second kind and of first order. For completeness, we denote that the analytical estimation (6) has been obtained under these conditions: we consider a sufficient amount of particles on the ring, number of cells should be significantly larger than number of particles and finally the analyzed region of the unit circle should be sufficiently far from segment boundaries.

4. Numerical representation of the MSCT-model

For numerical investigations of the above-described system we use the time-tested scheme based on the Monte Carlo methods, specifically the so-called Metropolis algorithm. Here we briefly summarize the corresponding simulation rules. In the first instance we generate an initial configuration of particle locations $\vec{\vartheta} = (\vartheta_1, \vartheta_2, \ldots, \vartheta_n)$. All the time we use the equidistant inter-particle angles. Thereafter all particle positions are repeatedly updated (25000 updates) according to the following rules:

- Using formula (4) the initial potential energy U_0 for the actual set of locations $\vec{\vartheta} = (\vartheta_1, \vartheta_2, \ldots, \vartheta_n)$ is calculated.

- We pick an index $\ell \in \{1,2,\dots,n\}$ at random.
- The value of the strain coefficient β_ℓ is adjusted to the actual localization ϑ_ℓ of the ℓth vehicle. Specifically:

$$\beta_\ell = \beta_0\, \theta(\vartheta_\ell)\, \theta(\varphi_c - \vartheta_\ell) + \beta_c\, \theta(\vartheta_\ell - \varphi_c)\, \theta(2\pi - \vartheta_\ell). \qquad (7)$$

- We draw a random number δ equally distributed in the interval $(0,1)$.
- The anticipated length of jump is discretized according to the formula

$$\omega = \frac{m}{2\pi}\left\lceil \frac{m}{n}\delta \right\rceil. \qquad (8)$$

- We compute an anticipated position $\vartheta'_\ell = \vartheta_\ell + \omega$ of the ℓth element. Because of singularity in the potential energy (4) the model particles cannot change their order. Therefore we accept ϑ'_ℓ only if $\vartheta'_\ell < \vartheta_{\ell-1}$.
- We calculate a value of potential energy U' determined for configuration $(\vartheta_1, \vartheta_2, \dots, \vartheta_{\ell-1}, \vartheta'_\ell, \vartheta_\ell, \dots, \vartheta_n)$.
- If $U' < U_0$ the ℓth particle position takes on a new value ϑ'_ℓ. If $U' \geq U_0$ then the Boltzmann factor $q = \exp[-\beta_\ell(U' - U_0)]$ should be compared with another random number g equally distributed in $(0,1)$. Provided that the inequality $q > g$ is fulfilled the ℓth particle position takes on the new value ϑ'_ℓ too. Otherwise, the original configuration $(\vartheta_1, \vartheta_2, \dots, \vartheta_n)$ remains unchanged.

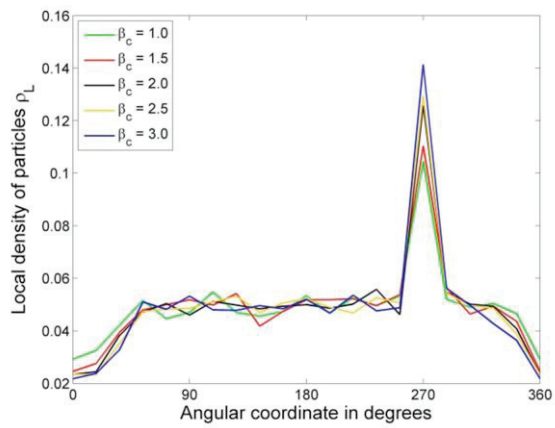

Figure 3. Density Profiles of Multi-Segment Thermal-like Cellular Model. We plot the local density of particles depending on angular position φ of the circular segment. The critical region is delimited by the angles $\varphi \in [270°, 360°)$ and weighted by the strain coefficient β_c (see legend). The strain coefficient in the unencumbered region $\varphi \in [0°, 270°)$ is zero. The global density of the analysed ensemble is 0.05.

The outlined scheme ensures a relaxation of ensemble into the steady state in which the socio-physical energy U fluctuates around a constant value being independent of an initial configuration of elements. After reaching such a probability-balance (i.e. after approximately 10000 updates of configuration) the ensemble lingers in this steady state until the simulation is interrupted.

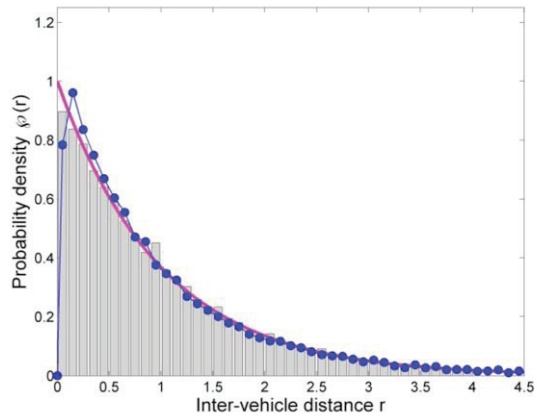

Figure 4. Distance Clearance Distribution inside the Free Zone. Bars represent the gaps among the subsequent particles of model (analysed inside the unencumbered region), whereas the bullets correspond to the inter-vehicle clearances measured on European freeways. Those real-road data have been chosen from the region of small densities, where traffic flows are fully fluent. The curve visualizes the analytical estimation (6) specified for $\beta = 0$.

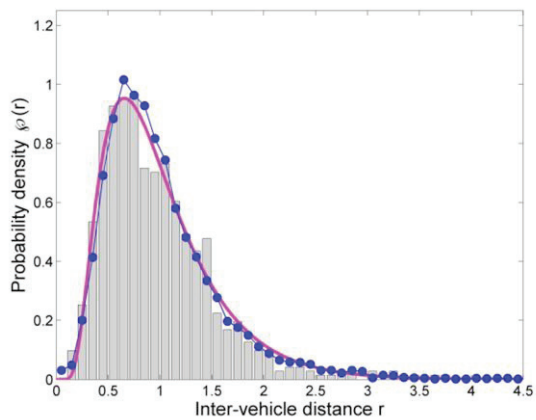

Figure 5. Distance Clearance Distribution inside the Critical Zone. Bars represent the gaps among the subsequent particles of model (analysed inside the critical region where $\beta_c = 1.0$), whereas the bullets correspond to the inter-vehicle clearances measured for the metastable traffic regimes, i.e for densities 35-38 veh/km/lane. The curve visualizes the analytical estimation (6) specified for $\beta = 1$.

5. Analysis the steady state of the MSCT-model

In this section we will try to analyze the steady state of the model defined. For all numerical simulations presented in our article we use the following settings: $n = 200, m = 4000, \varphi_c = 3\pi/2$, and finally $\beta_0 = 0$. Mental strain coefficient for the critical region (i.e. for region of angles $\varphi \in [\varphi_s, 2\pi)$) is varied (see text and figures below).

In the first instance we will investigate the macroscopic effects detected in the above-mentioned model. Surprisingly, in spite of thermal nature of the model the macroscopic analysis uncovers the effects of aggregation leading to the congested traffic states. This phenomenon is apparent when investigating the particle trajectories (see Figure 2). Note that the local traffic congestions are propagating through the whole circle, i.e they are detectable not only in the critical region but also in the free zone (where $\varphi \in [0, \varphi_s)$). Another way how to inspect the states of high saturations is to examine the local density of particle. For purposes of this observation the local and global densities are defined according to the formulae (9)

$$\rho_{\mathrm{L}}(\varphi) = \frac{1}{m}\,\mathrm{card}\left\{\vartheta_i \mid \varphi < \vartheta_i \leq \varphi + \frac{\pi}{10}\right\}, \qquad \rho_{\mathrm{G}} = \frac{n}{m}\,. \tag{9}$$

As visible in the figure 3, although the initial configuration of the model was uniform, i.e. the particle/vehicle locations were equidistant; the steady-state density is rapidly influenced by the varying values of psychological-pressure coefficient. Typically the effect of strong psychological strains causes the accumulation of particles in front of the critical region and leads to the intensive traffic saturation inside the segment. Evolving shock waves are distinguishable even inside the preceding free zone (where density of particles is smaller). This effect fully corresponds to the traffic reality.

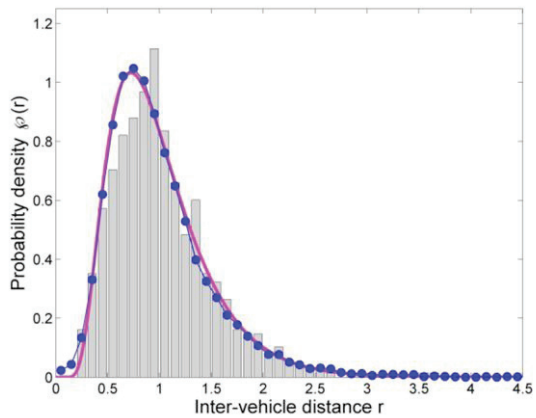

Figure 6. Distance Clearance Distribution inside the Critical Zone. Bars represent the gaps among the subsequent particles of model (analysed inside the critical region where $\beta_c = 1.5$), whereas the bullets correspond to the inter-vehicle clearances measured for the saturated traffic regimes, i.e. for densities 62-67 veh/km/lane. The curve visualizes the analytical estimation (6) specified for $\beta = 1.5$.

The interesting agreement between the MSCT-model presented and the real-road traffic systems can be found if investigating the corresponding microstructures. Here we are focused predominantly on the so-called clearance distribution, i.e. probability density for inter-vehicle gaps. In the figures 4-7 we explore such a statistical quantity in detail. Specifically, we compare the clearance distribution between the free zone and critical zone, where the mental strain coefficient is varying: $\beta_c = 1, \beta_c = 1.5, \beta_c = 2$, respectively. The detailed analysis of traffic data (gauged by induction double-loop detectors on European freeways) uncovers that clearances among vehicles are in excellent agreement with those measured in the steady state of our multi-segment model. To be concrete, an arbitrary regime of vehicular traffic can be identified with the specific choice of MSCT-parameters so that the relevant micro-statistics are very similar.

6. Summary and conclusions

We have introduced the multi-segment cellular thermal-like model (MSCT model) whose steady-state properties (both, micro-statistics and macro-effects) are in a good agreement with the relevant properties of vehicular streams. Comparisons between MSCT model and traffic reality clearly show that in spite of the thermal nature of the MSCT model, there is a direct link between the specific traffic states and associated steady states of MSCT model. Furthermore, such a correspondence has been achieved by applications of socio-physical approaches, when every agent of the system is limited by the agents occurring in his/her neighborhood (short-ranged repulsive interactions) and the subsequent decision making process of the agent is influenced by an individual level of mental strain. Reformulating those psychological aspects in terms of mathematical (or physical) rules we have obtained both, the numerical procedure leading to the steady state and analytical approximations for some statistical quantities describing the MSCT microstructure. This approach hopefully opens a new perspective in traffic modeling.

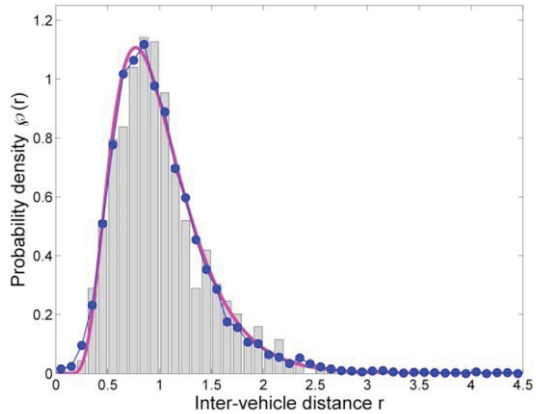

Figure 7. Distance Clearance Distribution inside the Critical Zone. Bars represent the gaps among the subsequent particles of model (analysed inside the critical region where $\beta_c = 2.0$), whereas the bullets correspond to the inter-vehicle clearances measured for the over-saturated traffic regimes, specifically for densities 77-82 veh/km/lane. The curve visualizes the analytical estimation (6) specified for $\beta = 2$.

Acknowledgements

This work was supported by the Ministry of Education, Youth and Sports of the Czech Republic within the projects LC06002 and MSM 6840770039. Additional support was provided by the project SGS 10/209/OHK4/2T/14.

References

Bogomolny E. B, Gerland U. & Schmit C. (2001). *Eur. Phys. J*. B 19, 121.

Chowdhury D., Santen L. & Schadschneider A. (2000). Statistical physics of vehicular traffic and some related systems. *Phys. Rep.*, 329, 199–369.

Derrida B., Domany E. & Mukamel. D. (1992). An exact solution of a one-dimensional asymmetric exclusion model with open boundaries. *Journal of Statistical Physics*, 69 3/4, 667–687.

Fukui M. & Ishibashi Y. (1996). Traffic flow in 1D cellular automaton model including cars moving with high speed. *J. Phys. Soc. Japan* 65 (6), 1868–1870.

Greenshields B. D. (1935). *Proceedings of the Highway Research Board* (Highway Research Board, Washington, D.C.), Vol. 14, 448.

Helbing D. (1995). *Quantitative Sociodynamics: Stochastic Methods and Models of Social Interaction Processes*, Kluwer Academic, Dordrecht.

Helbing D. (2001). *Rev. Mod. Phys*., 73, 1067.

Helbing D., Treiber M. & Kesting A. (2006). Understanding interarrival and interdeparture time statistics from interactions in queuing systems. *Physica A*, 363, 62–72.

Kerner B. S. (2004). *The Physics of Traffic*, Berlin, Springer.

Krbálek M. & Helbing D. (2004). Determination of interaction potentials in freeway traffic from steady-state statistics. *Physica A*, 333, 370–378.

Krbálek M. (2007). Equilibrium distributions in a thermodynamical traffic gas. *J. Phys. A: Math. Theor*., 40, 5813–5821.

Krbálek M. (2008). Inter-vehicle gap statistics on signal-controlled crossroads. *J. Phys. A: Math. Theor*., 41, 205004(1)–205004(8).

Krbálek M. & Šeba P. (2009). Spectral rigidity of vehicular streams (random matrix theory approach). *J. Phys. A: Math. Theor.* 42, 345001(1)–345001(10).

Mahnke R., Hinkel J., Kaupužs J. & Weber H. (2007). Application of thermodynamics to driven systems. *Eur. Phys. J. B*, 57, 463–471.

May A. D. (1990). *Traffic Flow Fundamentals*, Prentice Hall, Englewood Cliffs, NJ.

Nagel K. & Schreckenberg M. (1992). A cellular automaton model for freeway traffic. *J. Phys. I France* 2, 2221–2229.

Nishimura, Y., Cheon T. & Šeba P. (2006). Metastable congested states in multisegment traffic cellular automaton. *J. Phys. Soc. Jpn*., 75, 014801-014806.

Orosz G., Wilson R.E., Szalai R. & Stepan G. (2009). Exciting traffic jams: Nonlinear phenomena behind traffic jam formation on highways. *Phys. Rev. E*, 80, 046205(1)–046205(12).

Sopasakis A. (2004). Stochastic noise approach to traffic flow modeling. *Physica A* 342, 741–754.

Sugiyama Y., Fukui M., Kikuchi M., Hasebe K., Nakayama A., Nishinari K., Tadaki S. & Yukawa S. (2008). Traffic jams without bottlenecks–experimental evidence for the physical mechanism of the formation of a jam. *New Journal of Physics,* 10, 033001(1)–033001(8).